

Response of the near-surface carbonate system of the northwestern Arabian Sea to the southwest monsoon and related biological forcing

Ralf Lendt,¹ Helmuth Thomas,¹ Axel Hupe,² and Venugopalan Ittekkot³

Received 21 December 2000; revised 20 June 2002; accepted 16 April 2003; published 10 July 2003.

[1] Underway measurements of the CO₂ partial pressure ($p\text{CO}_2$) and the sea surface temperature were made in the northwestern Arabian Sea during late intermonsoon and southwest (SW) monsoon 1997. Additionally, dissolved inorganic carbon (DIC) and total alkalinity were analyzed from the surface and deeper waters. CO₂ fluxes between atmosphere and ocean surface were estimated. Monsoon-forced changes in the near-surface carbonate system became clearly visible a few weeks after onset of the SW monsoon. Because of the upwelling of CO₂-rich waters along the Omani coast, DIC and $p\text{CO}_2$ locally increased up to 2210 $\mu\text{mol kg}^{-1}$ and 715 μatm , respectively. The Arabian Sea thus acted as a CO₂ source during SW monsoon. Highest CO₂ fluxes of >150 $\text{mmol m}^{-2} \text{d}^{-1}$ were observed in the upwelling region off Oman, while the open Arabian Sea revealed relatively lower CO₂ fluxes but contributed more to the overall CO₂ release because of its larger area. Total CO₂ emissions from the Arabian Sea from May until August 1997 are estimated to amount 67.6 Tg C. The upwelling-induced impacts of biological activity on the carbon cycle were estimated by tracing freshly upwelled water along its transport way along the sea surface. The obtained CO₂ uptake by enhanced net community production (NCP) is ~ 3.6 times higher than the CO₂ emissions. In contrast to phosphate, upwelled nitrate apparently is consumed by NCP within a timescale of some 10 days, and the upwelling thus does not directly supply the central Arabian Sea with nitrate.

INDEX TERMS: 4806 Oceanography: Biological and Chemical: Carbon cycling; 4279 Oceanography: General: Upwelling and convergences; 4845 Oceanography: Biological and Chemical: Nutrients and nutrient cycling; **KEYWORDS:** Arabian Sea, carbon cycle, upwelling, CO₂ air-sea exchange, net community production

Citation: Lendt, R., H. Thomas, A. Hupe, and V. Ittekkot, Response of the near-surface carbonate system of the northwestern Arabian Sea to the southwest monsoon and related biological forcing, *J. Geophys. Res.*, 108(C7), 3222, doi:10.1029/2000JC000771, 2003.

1. Introduction

[2] Owing to the unique combination of climate, circulation, and geology, the northwestern Indian Ocean is characterized by several prominent features [Wyrski, 1971; Swallow, 1984; Zeitzschel and Gerlach, 1973]. The Arabian Sea is subject to strong seasonal monsoon-forced oscillations in atmospheric conditions which cause substantial physical, chemical, and biological changes in the upper layers of the water column. The phytoplankton new production is triggered by the upwelling of nutrient-rich waters along the Omani coast during the southwest (SW) monsoon period [Qasim, 1977, 1982] and by mixed layer deepening due to winter cooling and convective mixing. Large phytoplankton blooms during the summer period, dominated by

diatom species [Latasa and Bidigare, 1998], lead to an enhanced export pulse of particulate organic carbon (POC) to the deep sea via the biological pump [Haake et al., 1993]. The particle aggregation and their consecutive export are favored by the input of dust, which accelerates the downward flux of suspended matter [Ittekkot, 1991, 1993]. On the other hand, the biological CO₂ drawdown is counteracted by outgassing of CO₂ from upwelled thermocline waters, making the Arabian Sea a source for atmospheric CO₂ [e.g., George et al., 1994; Körtzinger et al., 1997]. Another characteristic feature of the Arabian Sea is an intense oxygen minimum zone (OMZ), containing $<5 \mu\text{mol kg}^{-1}$ O₂ established at middepth (150–1200 m) northward of 12°N and eastward of 56°E [e.g., Naqvi, 1987; Mantoura et al., 1993]. In waters of initially low O₂ content moderate oxygen consumption by organic matter remineralization maintains the OMZ [Olson et al., 1993].

[3] Our study focuses on monsoon-induced impacts on the carbon cycle of the upper 500 m as observed during the transition from late intermonsoon to SW monsoon 1997. We briefly describe the relevant observations. In order to investigate the impact of upwelling processes, notably of nutrient input from below the mixed layer, on

¹Department of Marine Chemistry and Geology, Royal Netherlands Institute for Sea Research (NIOZ), Texel, Netherlands.

²Institute of Biogeochemistry and Marine Chemistry, University of Hamburg, Hamburg, Germany.

³Centre for Tropical Marine Ecology, Bremen, Germany.

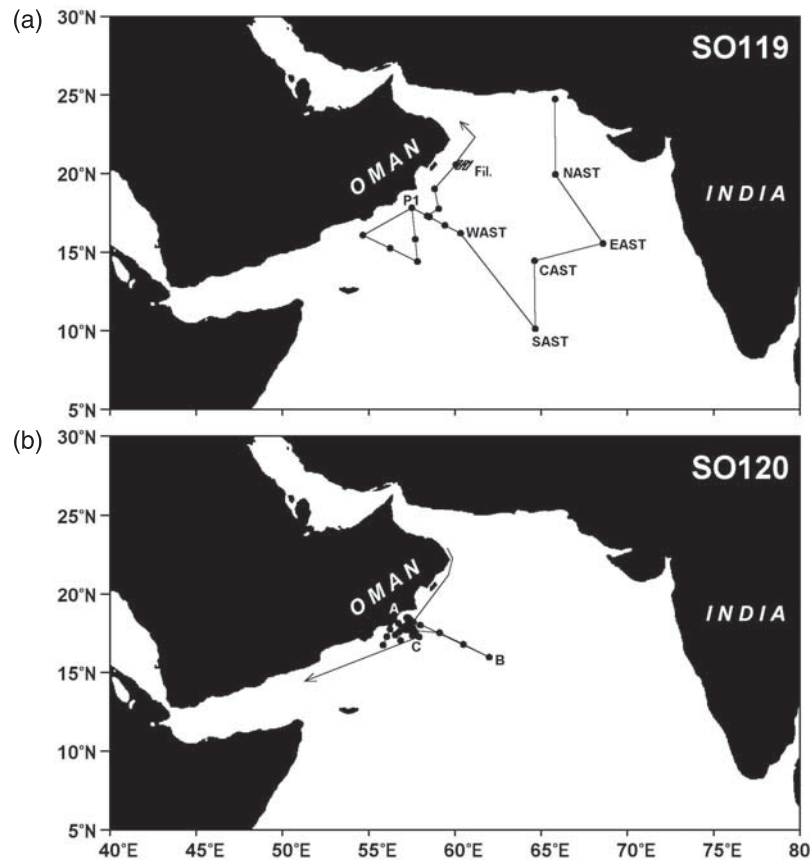


Figure 1. Cruise tracks and locations of CTD stations of German JGOFS cruises (a) SO119 and (b) SO120. The arrows indicate the direction of the ship's track.

the carbon cycle and thus the CO₂ source function of the Arabian Sea we introduce a procedure to obtain initial conditions of the upwelled water. The reconstructed source depths and the transport history of the upwelled waters enable a detailed description of processes governing the carbon budget at the surface. This finally allows estimation of the biological CO₂ drawdown induced by nutrient upwelling and the consequential impacts on the CO₂ air-sea exchange in the upwelling zone off Oman during SW monsoon.

2. Data

[4] The data presented here were collected on R.V. SONNE cruises SO119 (5 December to 6 October 1997) and SO120 (6–7 December 1997) within the German contribution to the Joint Global Ocean Flux Study (JGOFS) (Figure 1). The CO₂ partial pressure ($p\text{CO}_2$) in surface seawater and the atmospheric $p\text{CO}_2$ were recorded as one minute means using an automated system similar to the one described by Körtzinger *et al.* [1996]. The NDIR detector (LicorTM 6262) was calibrated every 12 hours using CO₂ free nitrogen as zero gas and two gas standards (CO₂ in natural air; 355.81 and 450.08 ppmv, provided by NOAA-CMDL, Boulder, CO, USA). The accuracy of $p\text{CO}_2$ measurements ranged between ± 1 ppmv according to the given concentrations of the standard

gases of 350 and 450 ppmv. The equilibrator of the $p\text{CO}_2$ system was supplied with a continuous, bubble-free stream of seawater (2 L min^{-1}) which was pumped from 6 m beneath the sea surface at a total flow rate of 40 L min^{-1} . Atmospheric $p\text{CO}_2$ measurements were performed every 2 hours. The clean air was sampled at the ship's bow mast and passed the system at a flow rate of about 1 L min^{-1} . The $p\text{CO}_2$ data are given for 100% humidity at the air-sea interface. Taking into account the observed slight warming of seawater between sample inlet and equilibrator of $0.5 \pm 0.1^\circ\text{C}$, $p\text{CO}_2$ was corrected to in situ seawater temperature. Temperature and salinity were recorded from the ship's thermosalinograph. Salinity measurements were calibrated vs. Autosal (GUILDLINETM) samples and temperature vs. CTD measurements, respectively. All calculations and corrections which were used to convert the raw CO₂ mole fraction into final $p\text{CO}_2$ values are described in detail by Department of Energy (DOE) [1994].

[5] Samples for total dissolved inorganic carbon (DIC) and total alkalinity (TA) were taken from the continuous pump system as well. Additionally, samples were taken from the CTD-Rosette equipped with 10 L Niskin bottles at various stations. DIC concentrations of seawater were determined using the coulometric technique according to Johnson *et al.* [1993] and are given as the average of three replicates of each sample. TA was measured with a

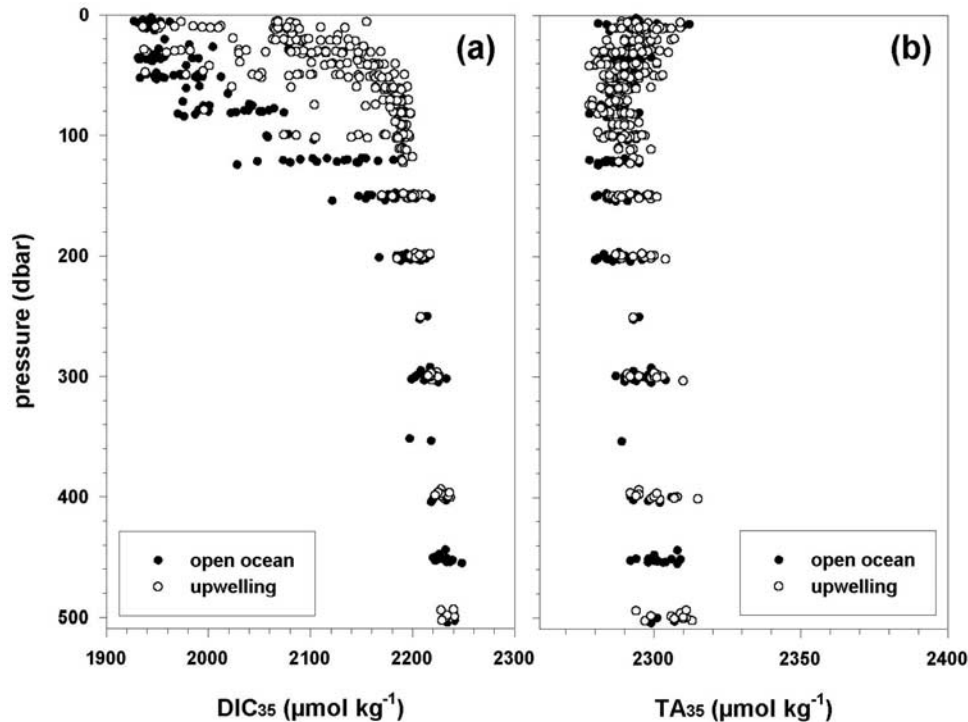


Figure 2. Vertical distributions of (a) normalized DIC ($\text{DIC} \times 35/S$) and (b) normalized TA ($\text{TA} \times 35/S$) in the upper 500 m of the water column on all stations during SO119 and SO120. Solid circles mark samples from the open ocean and samples from the coastal zone taken before upwelling; open circles mark samples from the coastal zone during upwelling.

potentiometric titration with a closed cell, using hydrochloric acid [Almgren *et al.*, 1983; Bradshaw and Brewer, 1988a, 1988b; Dickson, 1981]. The titration alkalinity was calculated from the titration curve using the curve fitting procedure of Campbell and Millero [1994]. Both methods were calibrated twice a day with certified reference material (CRM, batch 35, $\text{DIC} = 2111.62 \mu\text{mol kg}^{-1}$ and $\text{TA} = 2354.05 \mu\text{mol kg}^{-1}$) provided by A. Dickson (Scripps Institution of Oceanography, La Jolla, CA, USA). The overall uncertainty of the DIC and the TA measurements were derived from the comparison of the CRM measurement with the certified values and were $\pm 2 \mu\text{mol kg}^{-1}$ for DIC and $\pm 3.5 \mu\text{mol kg}^{-1}$ for TA, respectively. Nutrient concentrations were measured according to Grasshoff *et al.* [1983]. To achieve better data coverage for the whole Arabian Sea, data of two cruises obtained during the US WOCE program (WOCE N1, August 1995) and during the US JGOFS Arabian Sea Process Study (TTN#49, July/August 1995) were incorporated in our analysis.

3. Observations

3.1. Upper Water Column Properties

[6] The distributions of normalized DIC ($\text{DIC}_{35} = \text{DIC}/S \times 35$) and TA ($\text{TA}_{35} = \text{TA}/S \times 35$) within the upper 500 m of the water column are shown in Figures 2a and 2b. Normalizing DIC and TA to a constant salinity of 35 excludes changes in their concentrations due to variations in salinity. Thus variations in DIC_{35} and TA_{35} can be

assigned to biological processes such as photosynthetic CO₂ uptake, remineralization of organic matter, formation of calcium carbonate, dissolution of calcium carbonate (Aragonite) as well as to the air-sea exchange of CO₂. In order to underline the monsoon-induced changes, the samples shown in Figure 2 are separated into two groups: the open ocean and the coastal area samples before upwelling and, second, the coastal area samples during upwelling.

[7] DIC_{35} ranges from 1940 to 1970 $\mu\text{mol kg}^{-1}$ in the surface waters of the oligotrophic open Arabian Sea, then rapidly increases by about 200 $\mu\text{mol kg}^{-1}$ in the upper 200 m because of remineralization of organic material to a mean value of 2235 $\mu\text{mol kg}^{-1}$ at 500 m depth. In contrast, near-surface values of DIC_{35} in the upwelling area off Oman are elevated to an average of 2100 $\mu\text{mol kg}^{-1}$ by the supply of CO₂-rich deeper water. Between 110 and 120 m the DIC_{35} values of the upwelling samples are similar to those of deeper open ocean waters, implying the origin of upwelling is at this depth or below. Below 120 m, the profiles of DIC_{35} both from the upwelling condition and from the open ocean are similar. Somewhat lower DIC_{35} concentrations in the upper 120 m of the upwelling region probably are because of both the lower upwelling depth at the beginning of cruise SO120, when upwelling was not fully evolved, and the enhanced primary production in the euphotic zone fueled by high nutrient availability. Normalized alkalinity generally ranges between 2280 and 2320 $\mu\text{mol kg}^{-1}$ within the upper 500 m indicating that in this depth range no processes except changes in salinity

Table 1. Mean SST, DIC, DIC₃₅, TA, TA₃₅, and $p\text{CO}_2$ as Measured on German JGOFS Cruises SO119 and SO120 During Transition From Intermonsoon to SW Monsoon 1997

	SST, °C	DIC, $\mu\text{mol kg}^{-1}$	DIC ₃₅ , $\mu\text{mol kg}^{-1}$	TA, $\mu\text{mol kg}^{-1}$	TA ₃₅ , $\mu\text{mol kg}^{-1}$	$p\text{CO}_2$, μatm
Coastal region SO119	28	2030	1940	2390	2298	400
Open ocean SO119	30	1990	1940	2380	2298	385
Coastal region SO120	23.5	2140	2090	2350	2298	580
Open ocean SO120	28.5	2010	1950	2390	2298	390

affect TA significantly. Consequently TA is barely influenced by upwelling.

3.2. Surface Water Properties

[8] Hourly means of continuous sea surface temperature (SST), wind speed and $p\text{CO}_2$ measurements, as well as surface DIC, TA values along the tracks of German JGOFS cruises SO119 and SO120 are summarized in Table 1 and Figure 3. During the first ten days of SO119, a SST between 29° and 30°C was observed in the oligotrophic Northern

and central Arabian Sea accompanied by $p\text{CO}_2$ values ranging from 380 to 400 μatm (Figure 3a). The moderate CO₂ supersaturation with respect to the atmosphere of 40 to 60 μatm (mean $p\text{CO}_{2\text{air}} = 349 \mu\text{atm}$) is mainly a result of the general warming of the ocean surface at the end of the intermonsoon. After passing station P1, sudden drops in SST down to 26°C indicated initial upwelling structures a few days after the onset of the SW monsoon (24.05.1997) near the coast. These structures exhibited no significant raise in $p\text{CO}_2$. Surface DIC and TA (Figure 3b) ranged from 1960 to 2040 $\mu\text{mol kg}^{-1}$ and from 2320 to 2405 $\mu\text{mol kg}^{-1}$, respectively. The low concentrations near station SAST in the central Arabian Sea can be attributed to the low surface salinity between 35.1 and 35.5 in this region. DIC₃₅ and TA₃₅ exhibit constant values around 2040 and 2300 $\mu\text{mol kg}^{-1}$, respectively and indicate that the changes in DIC and TA are due to hydrographic variations. The first days of cruise SO120 were marked by small-scale variability in SST and $p\text{CO}_2$ when several upwelling structures were crossed on various transects parallel to and toward the Omani coast. SST locally decreased by 6°C and $p\text{CO}_2$ shows variations of

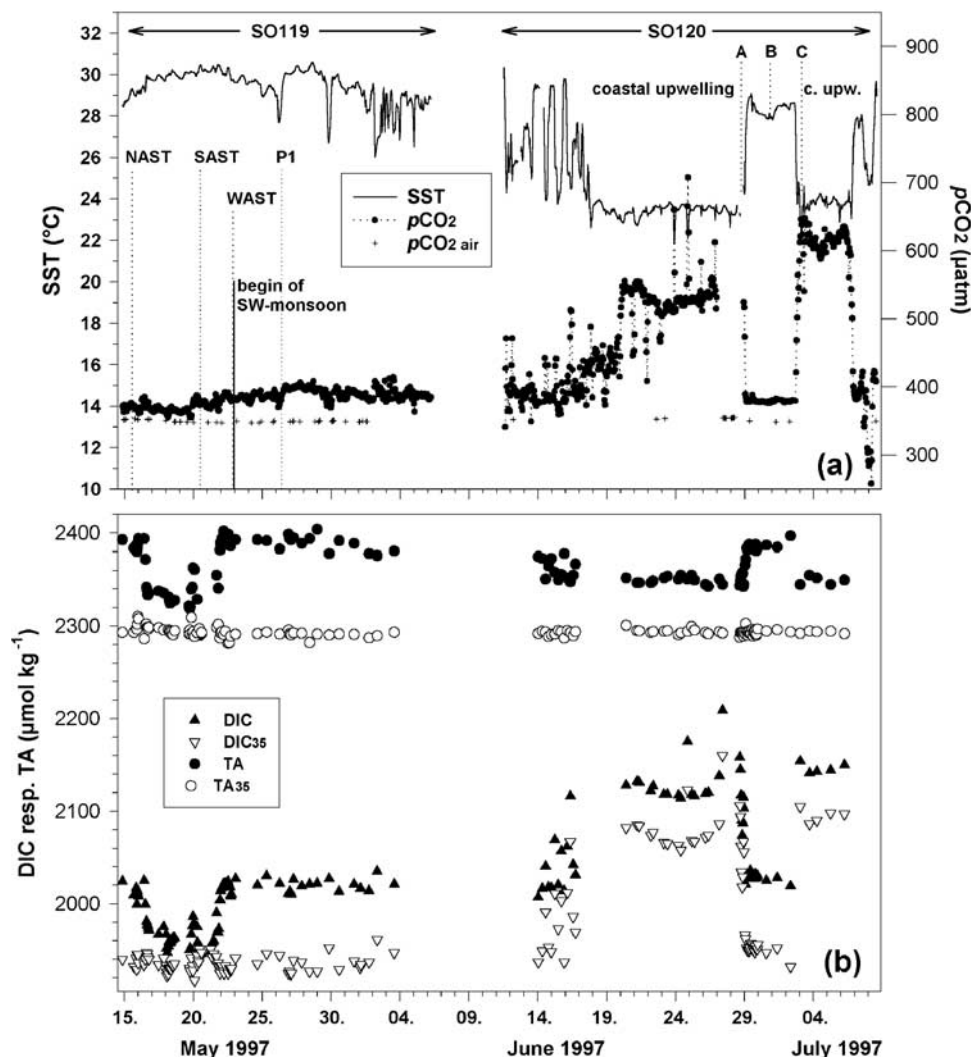


Figure 3. Hourly means of (a) sea surface temperature, seawater $p\text{CO}_2$, and atmospheric $p\text{CO}_2$ ($p\text{CO}_{2\text{air}}$) and (b) DIC, normalized DIC (DIC₃₅), TA, and normalized TA (TA₃₅) during cruises SO119 and SO120. Main stations and remarkable cruise features are marked for better orientation (compare with Figure 1).

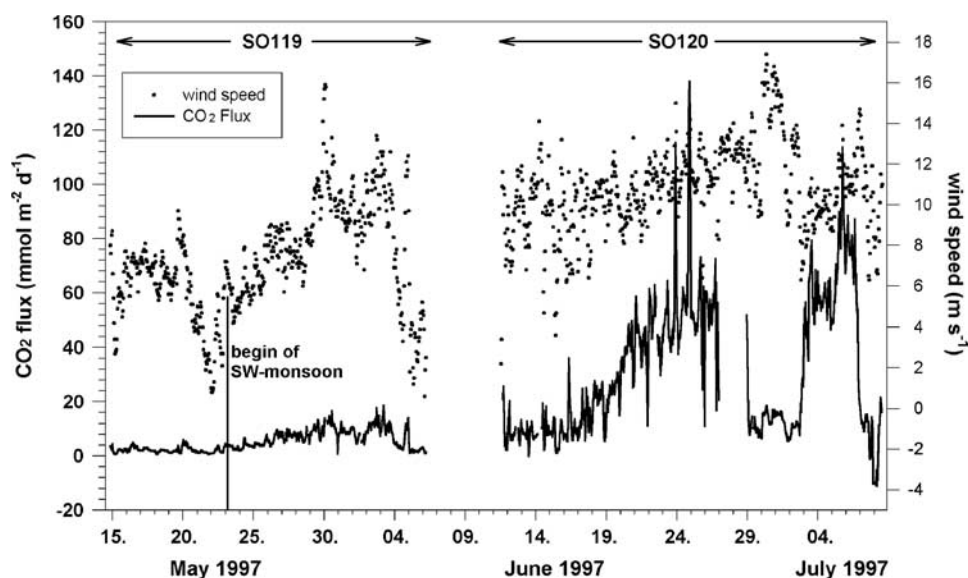


Figure 4. Wind speed and CO₂ flux between ocean and atmosphere during cruises SO119 and SO120. Flux calculations are based on hourly means of $p\text{CO}_2$ and wind speed. Positive values indicate CO₂ flux into the atmosphere; negative values represent CO₂ uptake by the ocean.

more than 100 μatm reaching maximum values of 500 μatm in colder water. During a drift study between 18.6. and 29.6.1997 the monsoon-forced changes in the surface CO₂ system became clearly visible. The upwelling of cold (SST = 23°–24°C) CO₂-rich water increased $p\text{CO}_2$ and DIC concentrations to mean values of 540 μatm and 2120 $\mu\text{mol kg}^{-1}$. Maximum values of DIC (2210 $\mu\text{mol kg}^{-1}$) were found 40 km off the coast (25.6.1997). Here, the upward transport of high DIC, low alkalinity water (Figure 3b) lead to a $p\text{CO}_2$ increase up to 710 μatm . Later (7 April to 7 July 1997) $p\text{CO}_2$ and DIC were elevated to mean values of >660 μatm and 2140 $\mu\text{mol kg}^{-1}$ respectively, reflecting increased upwelling intensity and upwelling depths as well as warming of the upwelled water during its exposure to the atmosphere.

[9] On a transect to the open Arabian Sea (A-B-C) a constant $p\text{CO}_2$ of 390 μatm and DIC of 2020 $\mu\text{mol kg}^{-1}$ were observed. These results agree with the observations during SO119 at the end of intermonsoon and show that the early SW monsoon has no significant effect on the surface distributions of both parameters in this region.

[10] Alkalinity concentrations in the upper 500 m are mainly affected by variations in salinity. As a result, here the TA₃₅ concentrations remain nearly constant (Figure 2b) and, taking into account an upwelling depth of 130 m as discussed later, TA₃₅ remains unchanged by upwelling processes and shows constant surface concentrations of $2300 \pm 5 \mu\text{mol kg}^{-1}$ in the entire northwestern and central Arabian Sea.

4. Results and Discussion

4.1. Air-Sea Flux of CO₂

[11] On the basis of $p\text{CO}_2$, SST and wind speed the CO₂ flux between the atmosphere and the ocean was calculated using the transfer coefficients of Wanninkhof [1992]. The results of the flux calculations during SO119 and SO120 are

shown in Figure 4. During the first 12 days of SO119 (15.5.–27.5.1997) a moderate CO₂ supersaturation and a mean wind speed between 5 and 10 m s^{-1} lead to a mean CO₂ flux of 5 $\text{mmol m}^{-2} \text{d}^{-1}$, whereas fluxes increased up to 15 $\text{mmol m}^{-2} \text{d}^{-1}$ between 27.5. and 4.6.1997. These higher fluxes can be mainly attributed to higher wind speed related to the beginning of SW monsoon because no significant change in $p\text{CO}_2$ was observed during this period (Figure 3a). Near the coast enhanced CO₂ fluxes of 40–50 $\text{mmol m}^{-2} \text{d}^{-1}$ were observed from 12.6. to 27.6.1997 which are related to increased $p\text{CO}_2$ of >500 μatm . Strong CO₂ emissions from the upwelling area located 40 km offshore are indicated by a maximum flux to the atmosphere of 140 $\text{mmol m}^{-2} \text{d}^{-1}$ driven by high $p\text{CO}_2$ values of 710 μatm . During the transect to the open Arabian Sea (29.6.–3.7.1997) the CO₂ fluxes decreased to 15 $\text{mmol m}^{-2} \text{d}^{-1}$ because of a drop in $p\text{CO}_2$. This value represents the background value in the open Arabian Sea during SW monsoon. Returning to the upwelling area, CO₂ fluxes were elevated to a mean value 60–80 $\text{mmol m}^{-2} \text{d}^{-1}$ related to increased $p\text{CO}_2$ of 600 μatm in average. West of the upwelling (8.7.1997) negative fluxes of $-15 \text{mmol m}^{-2} \text{d}^{-1}$ imply strong oceanic CO₂ uptake because of primary production.

[12] In order to estimate the CO₂ emissions from the Arabian Sea for one SW monsoon season, the calculated CO₂ fluxes were interpolated onto a $1^\circ \times 1^\circ$ grid. In order to achieve a better data coverage for the whole Arabian Sea, data of two cruises from 1995, one from the US WOCE program (WOCE N1, August 1995) and one from the US JGOFS Arabian Sea Process Study (TTN#49, July/August 1995) were included in our estimates (Figure 5). Our investigations of 1997 indicated that early SW monsoon causes no significant changes in $p\text{CO}_2$ far from the coastal region. Hence we suggest, that the open Arabian Sea data from SO119 represent the $p\text{CO}_2$ of May, June and July. The data from US WOCE cruise N1 were used

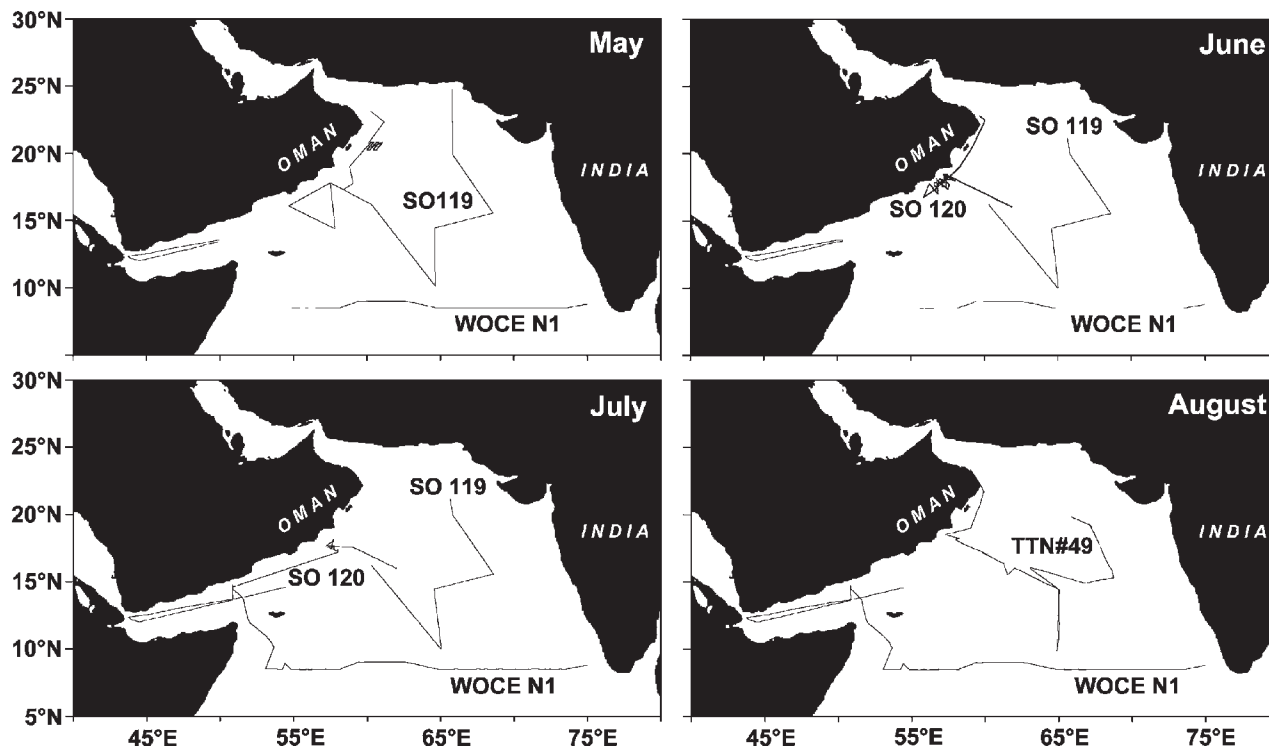


Figure 5. Maps of cruises that were used to estimate the CO₂ emissions from the Arabian Sea.

to calculate CO₂ fluxes from the southern Arabian Sea for May to August.

[13] The temporal development of the coastal upwelling is shown by interpolated CO₂ fluxes in Figure 6 and Table 2. During May the distribution of CO₂ flux is rather uniform throughout the whole investigation area. CO₂ fluxes from the coastal region into the atmosphere increased in the following month, reaching their maximum of 45 mmol m⁻² d⁻¹ in July. The extension of the isolines to the open Arabian Sea indicates higher CO₂ fluxes during June, July and August because of to increasing wind speed in the region of the Findlater jet and 2. spreading of the CO₂-rich upwelling water.

[14] These results emphasize the role of the Arabian Sea as a CO₂ source during SW monsoon as reported earlier for example by Somasundar *et al.* [1990], George *et al.* [1994], Körtzinger *et al.* [1997], Sarma *et al.* [1998], and Goyet *et al.* [1998]. The open Arabian Sea contributes 83% to the regional CO₂ emissions of 67.6 Tg C because of its large area (96% of the total area). Here, CO₂ exchange is mainly forced by the higher wind speeds during the monsoon and rather driven by the pCO₂ difference between surface water and atmosphere which did not increase significantly during the investigation time (Figure 3). The coastal upwelling waters are marked by mean CO₂ fluxes exceeding the fluxes in the open Arabian Sea three to four times, however because of the relatively smaller coastal area (4% of total) these fluxes contributed only 17% to the CO₂ source effect. It should be reminded here that in our study the upwelling areas southwest off India have not been considered because of which our results might be seen as lower bound or a slight underestimation of the CO₂ release of the Arabian Sea to the

atmosphere. Our overall estimates are in reasonable agreement with the results of Körtzinger *et al.* [1997]. If we compare our estimate with the annual emissions of 74 Tg C a⁻¹ as reported by Somasundar *et al.* [1990] and 69–79 Tg C a⁻¹ [George *et al.*, 1994], about 85% of the CO₂ emissions would occur during SW monsoon. However, as mentioned by George *et al.* [1994] their estimate is based only on intermonsoon data and therefore might tend to underestimate CO₂ fluxes in a highly variable region as the Arabian Sea. The great discrepancy between the latter investigations and the results of Goyet *et al.* [1998] reporting only 7 Tg C a⁻¹ for an area of 1,270,000 km² remains unclear. A possible explanation might be the different data interpolation techniques or a lack in considering biological processes in the latter work [see Sarma *et al.*, 1998].

4.2. Biological CO₂ Drawdown

[15] Upwelling zones are known as areas of nutrient enrichment and hence extensive primary production [e.g., Brock *et al.*, 1991; Brink *et al.*, 1998]. Brink *et al.* [1995] estimated their contribution to global oceanic new production to be 80–90%. Biological processes thus significantly affect the CO₂ properties in upwelling regions. In order to assess the impact of primary production driven by a coastal upwelling event on the carbon cycle, we develop a DIC budget for an upwelled water body. The hydrochemical properties of the water body were traced during repeated sections (Figure 7; see also Figure 1b, section A to B) as it moved offshore from the upwelling origin into the open Arabian Sea. Taking into consideration first the initial conditions for the water body at the time and location of the upwelling event and second the time history of this

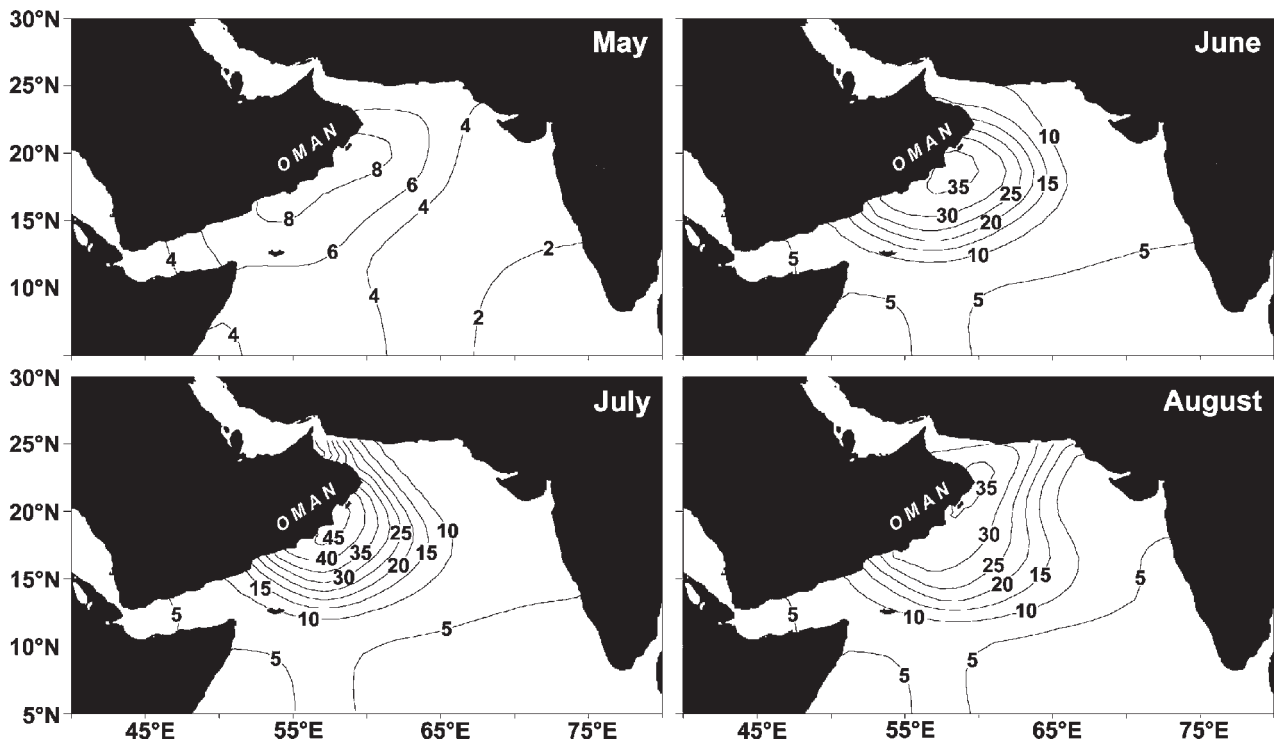


Figure 6. Interpolated CO₂ fluxes from the Arabian Sea during May, June, July, and August 1997.

water body at the surface, the above hydrochemical properties allow assessment of the relevant carbon cycle processes along its transport path.

[16] The depth of origin of the upwelled waters is required in order to identify its “initial” hydrochemical properties (DIC, Nutrients and T, S). To follow the carbon cycle processes in the upwelled water body transported at the surface, a measure of the water body’s history (life time) is required. We estimate this life time with reference to the water transport velocity observed during the present investigations.

[17] The upwelling origin depth was estimated to approximately 130 m by comparing depth profiles of salinity which were measured on the Omani shelf during cruise SO119 before the onset of upwelling and SO120 when upwelling was fully developed (Figure 8a). The DIC upwelling concentration was estimated with reference to the observed

depth/DIC relationship (Figure 2a). The corresponding “initial” DIC (DIC_{INI}) concentration was finally derived from a quadratic curve fit (Figure 8b) and determined to 2210 $\mu\text{mol kg}^{-1}$ (Table 3a). This value corresponds well with the highest measured surface DIC (Figures 2 and 3) near the coast which implies that freshly upwelled water was encountered at this location.

[18] In order to estimate the offshore transport velocity, SST measurements of two transects (Figure 9) one from the coast to the open ocean (transect 1, solid line) and one from the open ocean back to the coast (transect 2, dotted line) were compared. Figure 9 shows generally decreasing temperature toward the coast and the upwelling front which moved 38 km offshore within 76 hours lying between the observations of the two transects. The resulting velocity of 0.14 m s^{-1} or 12 km d^{-1} is in reasonable agreement with 3D

Table 2. Means of Wind Speed, SST, $\Delta p\text{CO}_2$, CO₂ Flux, and the Resulting CO₂ Emissions in Tg C (1 Tg = 10^{12} g) From the Arabian Sea During the SW Monsoon Season 1997^a

Region	Area, km ²	Mean Wind Speed, m s ⁻¹	Mean SST, °C	Mean $\Delta p\text{CO}_2$, μatm	Mean CO ₂ Flux, mmol m ⁻² d ⁻¹	CO ₂ Emissions, Tg C
Upwelling May	223,000	6.4	27.9	43	6.5	0.7
Open ocean May	4,953,000	5.6	29.8	24	4.0	7.4
Upwelling June	223,000	10.4	23.5	156	32.4	2.7
Open ocean June	4,953,000	9.4	28.4	30	8.5	15.8
Upwelling July	223,000	10.1	23.8	260	38.6	3.2
Open ocean July 97	4,953,000	9.3	28.4	29	9.0	17.5
Upwelling August	223,000	9.7	23.3	203	30.4	2.5
Open ocean August	4,953,000	9.0	27.5	38	9.6	17.8
Total	5,176,000					67.6

^aCO₂ fluxes were calculated according to Wanninkhof [1992] with hourly means of wind speed.

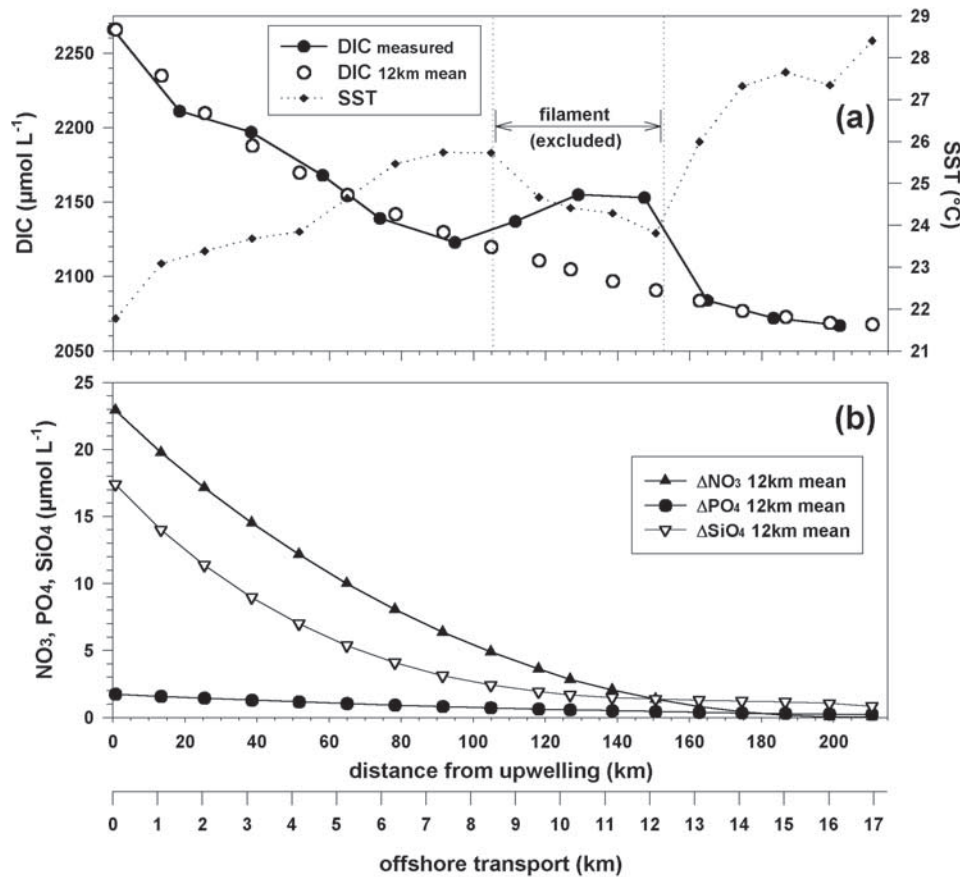


Figure 7. Horizontal distributions of (a) SST and DIC (measured and 12 km means) and (b) nutrients given as 12 km means on a surface transect from the coastal region to the open Arabian Sea. For convenience, the data are shown as function of both distance and time from the upwelling area in order to describe both the temporal and spatial development of the water body with time. A filament that had been passed between kilometers 110 and 160 (approximately day 8.5 until day 12.5) was excluded from calculations. The 12 km means were linearly interpolated in this section. Nutrient data were provided by C. Sellmer and K. v. Bröckel, Institute of Marine Research, University of Kiel, Kiel, Germany.

circulation model results (E. Maier-Reimer, personal communication). Taking into account the distance from the upwelling area and the above transport velocities it is now possible to determine, when a certain point on the transect (water body) had been brought to the surface by upwelling. Once having obtained both initial concentrations and time history of a water body the carbon and nutrient fluxes can be obtained from the differences between the observed and the initial concentrations.

[19] During transport the carbon budget of the water body is most notably governed by two processes, the CO₂ air-sea exchange and biological activity. Accordingly, the total change of DIC ($\Delta\text{DIC}_{\text{TOT}}$) comprises the changes because of CO₂ air-sea exchange ($\Delta\text{DIC}_{\text{FLUX}}$) and biological activity, i.e., net community production (NCP) or respiration ($\Delta\text{DIC}_{\text{BIO}}$) (equation (1a)). $\Delta\text{DIC}_{\text{TOT}}$ thereby is given as the difference between the initial value (DIC_{INI}) and the observation (DIC_{OBS}) (equation (1b)). The corresponding procedure has been applied to the nutrient (NUT) concentrations (NO₃, SiO₂, PO₄) (equation (1c) and Table 3a). The water body's time history and the daily averaged pCO₂ observations along the transect are used to assess the CO₂

air-sea exchange ($\Delta\text{DIC}_{\text{FLUX}}$) integrated for the period the water body has been in contact with the atmosphere. In order to assess the DIC loss related to degassing, CO₂ fluxes were integrated to the mixed layer depth (MLD) which was 25 m before onset of SW monsoon and less than 10 m when the upwelling was developed (Figure 8a, compare with Brock *et al.* [1991]). The CO₂ air-sea exchange coefficient (k_{ex}) has been calculated according to Wanninkhof [1992] (equation (1d)):

$$\Delta\text{DIC}_{\text{TOT}} = \Delta\text{DIC}_{\text{FLUX}} + \Delta\text{DIC}_{\text{BIO}} \quad (1a)$$

$$\Delta\text{DIC}_{\text{TOT}} = \text{DIC}_{\text{INI}} - \text{DIC}_{\text{OBS}} \quad (1b)$$

$$\Delta\text{NUT}_{\text{TOT}} = \text{NUT}_{\text{INI}} - \text{NUT}_{\text{OBS}} \quad (1c)$$

$$\Delta\text{DIC}_{\text{FLUX}} = \int \Delta p\text{CO}_2 k_{\text{ex}} dt * \text{MLD}^{-1} \quad (1d)$$

For further evaluation we used 12 km, i.e., daily averages of the pCO₂, DIC and nutrient data representing one-day

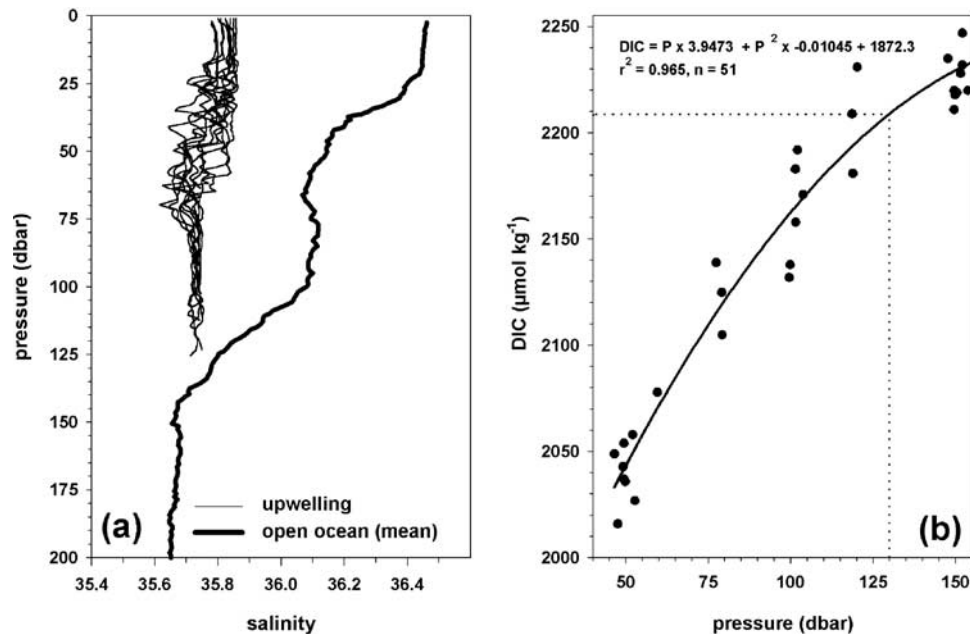


Figure 8. (a) Comparison between salinity profiles from the Omani shelf before (mean, thick line) and during (thin lines) upwelling, showing the origin of upwelling at approximately 130 m depth. (b) A quadratic curve fit was obtained from the correlation between DIC and depth. DIC values stem from CTD stations during the upwelling. The dotted line indicates the initial DIC concentration of $2210 \mu\text{mol kg}^{-1}$ at the estimated upwelling origin of 130 m depth.

transport in offshore direction (Figures 7a and 7b). According to (1a) the difference between $\Delta\text{DIC}_{\text{TOT}}$ and $\Delta\text{DIC}_{\text{FLUX}}$ can be attributed to biological activity ($\Delta\text{DIC}_{\text{BIO}}$). The obtained $\Delta\text{DIC}_{\text{TOT}}$, $\Delta\text{DIC}_{\text{FLUX}}$ and $\Delta\text{DIC}_{\text{BIO}}$ are summarized in Table 3b and Figure 10a. Because of the above integration over the mixed layer depth volumetric units will be applied in the further context.

[20] During 17 days of offshore transport, the surface DIC decrease amounts to approximately $200 \mu\text{mol L}^{-1}$ from its initial upwelling value of $2265 \mu\text{mol L}^{-1}$ to $2065 \mu\text{mol L}^{-1}$ (Figure 7a). In the coastal zone enhanced CO₂ release to the atmosphere up to $70 \text{ mmol m}^{-2} \text{ d}^{-1}$ caused by large $p\text{CO}_2$ differences between sea surface and atmosphere lead to a maximum DIC decrease. Moreover, near the coast intense primary production causes strongest biological CO₂ drawdown ($213 \text{ mmol m}^{-2} \text{ d}^{-1}$) and nutrient uptake (Figures 10a and 10b) as a result of the upwelling-induced high nutrient supply (initial upwelling concentrations: nitrate, $23 \mu\text{mol L}^{-1}$; phosphate, $1.8 \mu\text{mol L}^{-1}$; and silicate, $17.5 \mu\text{mol L}^{-1}$; Table 3a; compare Figure 7b). During the transport to the oligotrophic open ocean the CO₂ release to the atmosphere is reduced by decreasing surface DIC concentrations. This decrease has been caused by the CO₂ release itself and the biological CO₂ drawdown. The biological CO₂ drawdown in turn is diminished by the decreasing nutrient concentrations finally limiting primary production. In contrast to the $\Delta\text{DIC}_{\text{FLUX}}$, $\Delta\text{DIC}_{\text{BIO}}$ does not decrease continuously but shows another peak after 12 days, which might be an indication of a change in the phytoplankton community structure (see below). Over the 17 day period represented in Figure 10a, the total DIC loss due to biological processes is remarkably higher than the loss to the atmosphere which emphasizes the role of CO₂ uptake by primary production as

an important process in counteracting the CO₂ emissions caused by the upwelling of CO₂-rich water off Oman.

4.3. Nutrient Consumption and Its Relation to Carbon Uptake

[21] Figure 7b shows the surface distribution of nitrate (NO₃), phosphate (PO₄) and silicate (SiO₂) near the Omani coast given as 12 km means. All three parameters show enhanced concentrations of $23 \mu\text{mol L}^{-1}$, $2 \mu\text{mol L}^{-1}$ and $17.5 \mu\text{mol L}^{-1}$, respectively, near the coast. Nitrate concentrations decrease to near zero during 17 days offshore transport whereas phosphate and silicate concentrations decrease to 0.25 and $1.7 \mu\text{mol L}^{-1}$ in the open ocean. The stronger decrease in silicate during the first days implies a phytoplankton community dominated by diatoms near the coast as reported earlier by *Latasa and Bidigare* [1998].

[22] During the first four days $\Delta\text{C}/\Delta\text{N}$, $\Delta\text{C}/\Delta\text{P}$ and $\Delta\text{N}/\Delta\text{P}$ ratios (Figures 11a–11c) of 6.2 and 105.1 and 16.9 reflect the classical Redfield ratio for marine phytoplankton [*Redfield et al.*, 1963]. $\Delta\text{C}/\Delta\text{Si}$ and $\Delta\text{N}/\Delta\text{Si}$ (Figures 11d and 11e) amount to 5.4 and 0.9 respectively. The low $\Delta\text{N}/\Delta\text{Si}$ ratio provides evidence for a nearshore diatom bloom [*Brzezinski*, 1985; *Wilkerson and Dugdale*, 1996; *Latasa and Bidigare*, 1998]. Accordingly, 75% of the available

Table 3a. Initial Conditions of an Upwelled Water Body

Initial Conditions	Values
DIC, $\mu\text{mol L}^{-1}$	2265
NO ₃ , $\mu\text{mol L}^{-1}$	23
PO ₄ , $\mu\text{mol L}^{-1}$	1.8
SiO ₂ , $\mu\text{mol L}^{-1}$	17.5

Table 3b. Daily Changes in DIC, Total ($\Delta\text{DIC}_{\text{TOT}}$), Due to Air-Sea Exchange ($\Delta\text{DIC}_{\text{FLUX}}$) and Due to Net Community Production ($\Delta\text{DIC}_{\text{BIO}}$) and Daily Uptake of Nutrients in an Upwelling Water Body During Its Transport in Offshore Direction

Offshore Transport, days	Distance From Upwelling, km	$\Delta\text{DIC}_{\text{TOT}}$, mmol m ⁻² d ⁻¹	$\Delta\text{DIC}_{\text{FLUX}}$, mmol m ⁻² d ⁻¹	$\Delta\text{DIC}_{\text{BIO}}$, mmol m ⁻² d ⁻¹	ΔNO_3 , mmol m ⁻² d ⁻¹	ΔPO_4 , mmol m ⁻² d ⁻¹	ΔSiO_4 , mmol m ⁻² d ⁻¹
0	0	0	0	0	0	0	0
1	13.4	284.2	70.8	213.4	32.5	1.6	34.9
2	25.4	247.1	59.5	187.6	26.9	1.4	26.8
3	38.6	229.2	51.6	177.6	26.9	1.4	24.8
4	51.7	184.7	42.1	142.6	24.0	1.3	20.1
5	65.0	157.9	37.7	120.2	22.3	1.3	16.7
6	78.3	135	33.2	101.8	19.8	1.2	13.1
7	91.6	117.9	28.8	89.1	17.4	1.1	9.9
8	104.9	105.3	24.3	81	15.2	1.0	7.2
9	118.2	96.1	19.9	76.2	13.0	0.9	5.0
10	126.9	65.5	15.5	50	8.8	0.7	2.7
11	138.6	94.7	13.2	81.5	11.3	0.9	2.8
12	150.6	103.9	11	92.9	12.0	1.1	2.2
13	162.7	137.6	9.4	128.2	11.1	1.1	1.5
14	174.6	138.1	7.9	130.2	9.2	1.1	1.3
15	186.6	107.3	3.9	103.4	6.5	1.1	1.2
16	198.9	74.6	5.1	69.5	3.1	0.9	1.2
17	210.6	43.3	3.2	40.1	0.0	0.7	1.1
Total		2322.4	437.1	1885.3	260.0	18.9	172.6

silicate appears to be consumed within the first four days, but little silicate is depleted after this period. *Dugdale et al.* [1995] reported that the K_s (half saturation constant) for silicate uptake by coastal diatoms is high, which leads to limitation of diatom blooms, even if silicate concentrations are up to $2 \mu\text{mol L}^{-1}$. A transition from a diatom dominated phytoplankton community to one which is marked by non siliceous species during the “aging” of the upwelling water along its offshore trajectory path may have occurred between days 4 and 10. This would also explain the relatively low DIC uptake rates at day 10 in Figure 10a. $\Delta\text{C}/\Delta\text{Si}$ and $\Delta\text{N}/\Delta\text{Si}$ increase to 18 and 2.8. The decrease in $\Delta\text{C}/\Delta\text{P}$ to 77.2 and $\Delta\text{N}/\Delta\text{P}$ to 12.1 might imply “luxury consumption” of phosphorus [Droop, 1973; Thomas et al., 1999] at the beginning of a new bloom. The ongoing carbon and

phosphorus uptake (Figures 10a and 10b) under nitrate depleted conditions (Figure 7b) at day 17 might be a hint to nitrogen fixing organisms like cyanobacteria [Burkill et al., 1993].

[23] The depletion of NO_3 after 17 days also suggests that the coastal upwelling does not supply nitrate for large phytoplankton blooms in the central Arabian Sea which have been observed by CZCS images [e.g., Brock and McClain, 1992; Banse and McClain, 1986; Banse, 1994]. Rather open ocean upwelling, mixed layer deepening and filaments appear to be the main physical mechanisms of nitrate supply for these offshore blooms.

[24] Net community production rates (Figure 12) derived from our DIC loss estimates by integration over a MLD of 10 m amount a maximum of $2.6 \text{ g C m}^{-2} \text{ d}^{-1}$ and an

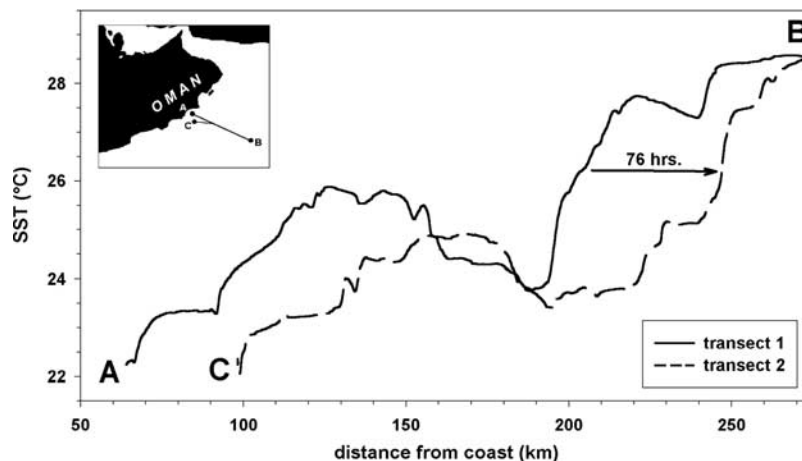


Figure 9. One minute means of SST on two transects, one from the coast to the open ocean (transect 1) and one from the open ocean to the coast (transect 2). Here 76 hours passed between the observations on the two transects, implying an offshore current velocity of 12 km d^{-1} .

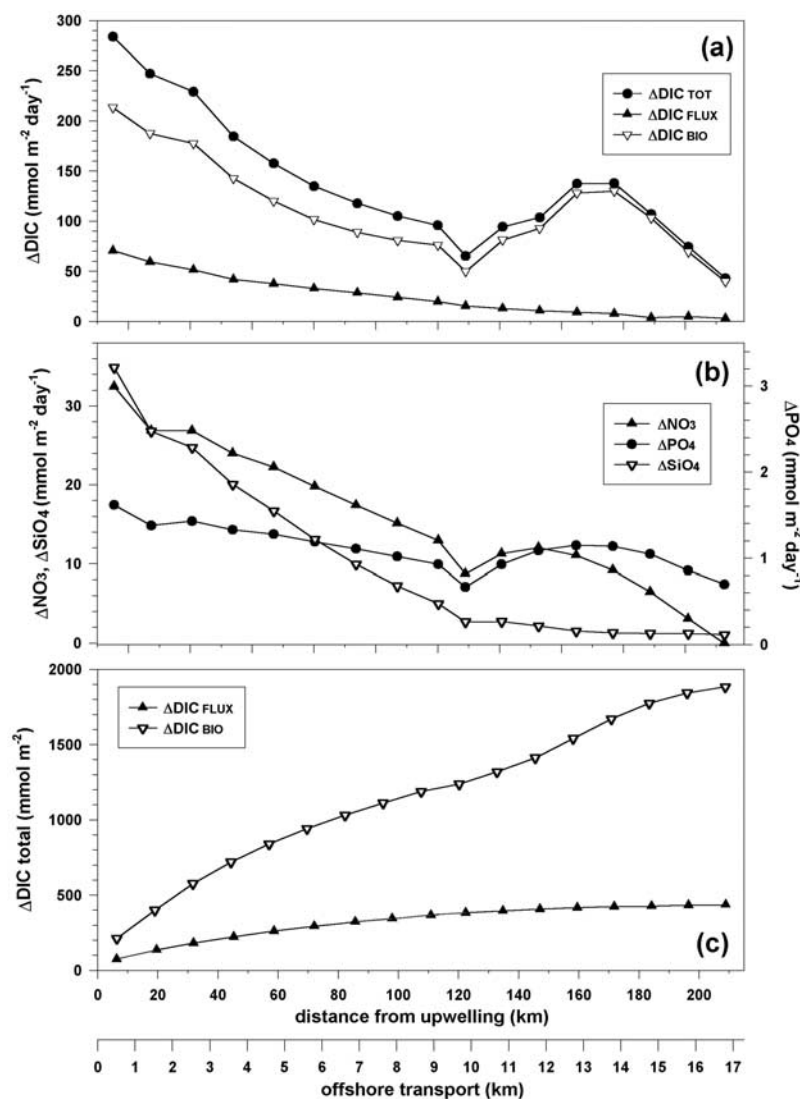


Figure 10. (a) Daily changes of DIC in upwelled water due to CO₂ air-sea exchange ($\Delta\text{DIC}_{\text{FLUX}}$) and due to biological CO₂ uptake ($\Delta\text{DIC}_{\text{BIO}}$), (b) daily changes in nutrients due to biological uptake, given as fluxes, and (c) cumulative changes of DIC in upwelling water during 17 days offshore transport. All data are taken from transect 1.

average of $1.39 \text{ g C m}^{-2} \text{ d}^{-1}$ in and near the upwelling area and are in good agreement with measured rates of *Owens et al.* [1993] and *Sellmer* [1999] as well as chlorophyll *a* measurements. The extrapolation of the mean production rate over the entire upwelling region ($223,000 \text{ km}^2$) yields a daily carbon fixation by NCP of 0.31 Tg C . Throughout the SW monsoon season 1997 (middle of May to end of August) a total of 33 Tg C was removed from the mixed layer to form organic matter. Thus the biological CO₂ uptake is 3.6 times higher than the CO₂ emissions from the upwelling area (9.1 Tg C), and hence, without the CO₂ drawdown by primary production, the CO₂ emissions from the upwelling could be much higher than reported above.

[25] We suggest that most of the organic material formed in the upwelling region is transported to the open Arabian Sea via eddies and filaments. These structures are known to be the primary mechanisms of horizontal offshore transport [e.g., *Brink et al.*, 1998] and show elevated

chlorophyll concentrations [*Bidigare et al.*, 1997] and complex biogeochemical forcing [*Lendt et al.*, 1999]. This appears to be in good agreement with export rates derived from sediment trap studies of *Haake et al.* [1993] and *Honjo et al.* [1999], which exhibit the peak of export at the end of SW monsoon.

5. Conclusions

[26] The Arabian Sea is a net source for CO₂ during SW monsoon. Maximum CO₂ flux to the atmosphere of $>150 \text{ mmol m}^{-2} \text{ d}^{-1}$ can be attributed to the transport of cold and CO₂-rich waters to the surface in the coastal upwelling off Oman. Surface waters in the open ocean region are moderately CO₂ supersaturated. Our estimates gave CO₂ emissions of 67.6 Tg C during the SW monsoon season 1997 (May to August). Processes controlling the carbon cycle during an upwelling event have

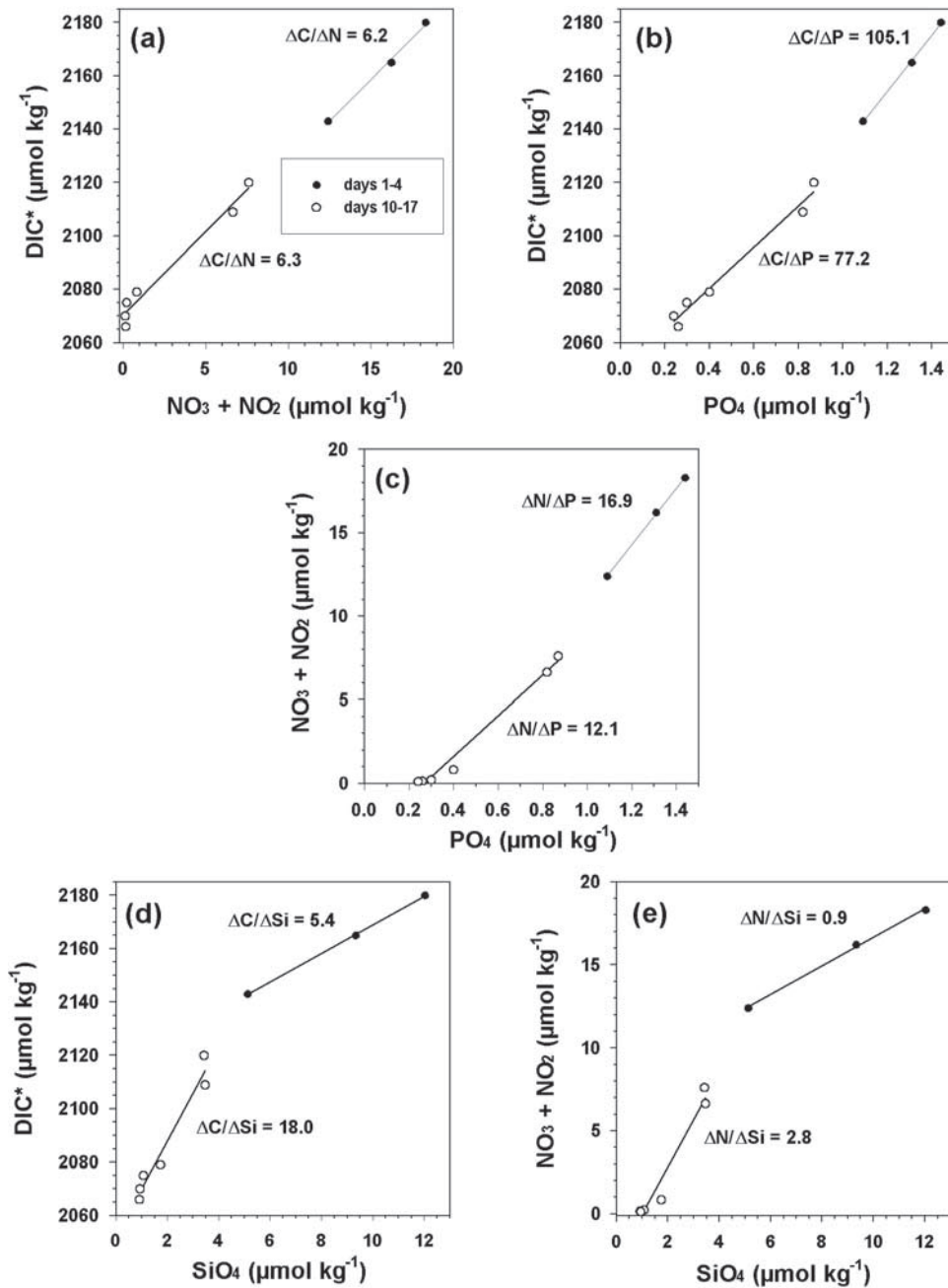


Figure 11. $\Delta\text{C}/\Delta\text{N}/\Delta\text{P}/\Delta\text{Si}$ uptake ratios derived from DIC and nutrient measurements on transect 1. DIC* represents the air-sea exchange-corrected DIC, which is changed by biological processes only ($\Delta\text{DIC}_{\text{BIO}}$).

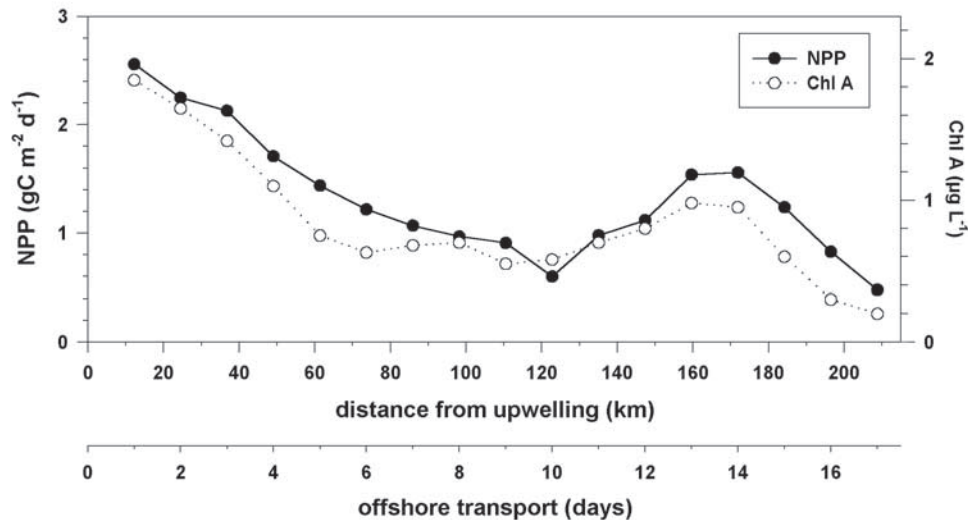


Figure 12. Net community production (NPP) rates derived from $\Delta\text{DIC}_{\text{BIO}}$ in comparison with measures on transect 1. Chlorophyll *a* data were provided by C. Sellmer and K. v. Bröckel, Institute of Marine Research, University of Kiel, Kiel, Germany.

been identified and quantified. The biological CO₂ uptake is 3.6 times higher than the CO₂ release to the atmosphere. The biological CO₂ uptake is thus an important process in counteracting CO₂ emissions from the upwelling area off Oman and small changes in biology may have strong impact on the CO₂ system in these regions. Upwelled nitrate is consumed by primary production within a few weeks on the trajectory path of the upwelling water and is apparently not exported to the open Arabian Sea.

[27] **Acknowledgments.** We wish to thank the crews of RV SONNE and all participants of cruises SO119 and SO120 for their kind support. We also wish to thank C. Sellmer and K. v. Bröckel for providing the nutrient and chlorophyll *a* data and E. Maier-Reimer for helpful discussion. We are deeply indebted to Christopher L. Sabine and Robert M. Key, Richard Barber, Catherine Goyet and the various other scientists providing Arabian sea data used in this work. The comments by an anonymous reviewer helped improve the manuscript significantly. Financial support of our research by the German Bundesministerium für Bildung und Forschung (BMBF), grant no. 03F0183A, is gratefully acknowledged.

References

- Almgren, T., D. Dyrssen, and S. Fonselius, Determination of alkalinity and total carbonate, in *Methods of Seawater Analysis*, edited by K. Grasshoff, M. Ehrhardt, and K. Kremling, Verl. Chem., Weinheim, Germany, 1983.
- Banse, K., Uptake of inorganic carbon and nitrate by marine plankton and the Redfield ratio, *Global Biogeochem. Cycles*, **8**, 81–84, 1994.
- Banse, K., and C. R. McClain, Winter blooms of phytoplankton in the Arabian Sea as observed by the Coastal Zone Color Scanner, *Mar. Ecol. Prog. Ser.*, **34**, 201–211, 1986.
- Bidigare, R. R., M. Latasa, Z. Johnson, R. T. Barber, C. C. Trees, and W. M. Balch, Observations of a *Synechococcus*-dominated cyclonic eddy in open-oceanic waters of the Arabian Sea, *Proc. SPIE Ocean Opt.*, **2963**, 260–265, 1997.
- Bradshaw, A. L., and P. G. Brewer, High precision measurements of alkalinity and total carbon dioxide in seawater by potentiometric titration: 1. Presence of unknown protolyte(s)?, *Mar. Chem.*, **23**, 69–86, 1988a.
- Bradshaw, A. L., and P. G. Brewer, High precision measurements of alkalinity and total carbon dioxide in seawater by potentiometric titration: 2. Measurements on standard solutions, *Mar. Chem.*, **24**, 155–162, 1988b.
- Brink, K. H., F. F. G. Abrantes, P. A. Bernal, R. C. Dugdale, M. Estrada, L. Hutchings, R. A. Jahnke, P. J. Müller, and R. L. Smith, How do coastal upwelling systems operate as integrated physical, chemical, and biological systems and influence the geological record? The role of physical processes in defining the spatial structures of biological and chemical variables, in *Upwelling in the Ocean—Modern Processes and Ancient Records*, edited by C. P. Summerhayes et al., pp. 103–124, John Wiley, New York, 1995.
- Brink, K. H., et al., Monsoons boost biological productivity in Arabian Sea, *EOS*, **79**, 165–169, 1998.
- Brock, J. C., and C. R. McClain, Interannual variability in phytoplankton blooms observed in the northwestern Arabian Sea during the southwest monsoon, *J. Geophys. Res.*, **97**, 733–750, 1992.
- Brock, J. C., C. R. McClain, M. E. Luther, and W. W. Hay, The phytoplankton bloom in the northwestern Arabian Sea during the southwest monsoon of 1979, *J. Geophys. Res.*, **96**, 20,623–20,642, 1991.
- Brzezinski, M. A., The Si:C:N ratio of marine diatoms: Interspecific variability and the effect of some environmental variables, *J. Phycol.*, **21**, 347–357, 1985.
- Burkill, P. H., R. J. A. Leakey, N. J. P. Owens, and R. F. C. Mantoura, *Synechococcus* and its importance to the microbial foodweb of the northwestern Indian Ocean, *Deep Sea Res., Part II*, **40**, 773–782, 1993.
- Campbell, D. W., and F. J. Millero, *Alkalinity Titration System Manual*, Rosenstiel Sch. of Mar. and Atmos. Sci., Univ. of Miami, Miami, Fla., 1994.
- Department of Energy (DOE), Handbook of Methods for the Analysis of the Various Parameters of the Carbon Dioxide System in Sea Water, version 2, edited by A. G. Dickson and C. Goyet, Oak Ridge Natl. Lab./Carbon Dioxide Inf. Anal. Cent., Oak Ridge, Tenn., 1994.
- Dickson, A. G., An exact definition of total alkalinity and a procedure for the estimation of alkalinity and total inorganic carbon from titration data, *Deep Sea Res., Part A*, **28**, 609–623, 1981.
- Droop, M. R., Some thoughts on nutrient limitation on algae, *J. Phycol.*, **9**, 264–272, 1973.
- Dugdale, R. C., F. P. Wilkerson, and H. J. Minas, The role of a silicate pump in driving new production, *Deep Sea Res., Part I*, **42**, 697–719, 1995.
- George, M. D., M. D. Kumar, S. W. A. Naqvi, S. Banerjee, P. V. Narvekar, S. N. de Sousa, and D. A. Jayakumar, A study of the carbon dioxide system in the northern Indian Ocean during premonsoon, *Mar. Chem.*, **47**, 243–254, 1994.
- Goyet, C., F. J. Millero, D. W. O’Sullivan, G. Eiseheid, S. J. McCue, and R. G. J. Bellerby, Temporal variations of pCO₂ in surface seawater of the Arabian Sea in 1995, *Deep Sea Res.*, **45**, 609–623, 1998.
- Grasshoff, K., M. Erhardt, and K. Kremling, *Methods of Seawater Analysis*, 2nd ed., Verl. Chem., Weinheim, Germany, 1983.
- Haake, B., V. Ittekkot, T. Rixen, V. Ramaswamy, R. R. Nair, and W. B. Curry, Seasonality and interannual variability of particle fluxes to the deep Arabian Sea, *Deep Sea Res., Part I*, **40**, 1323–1344, 1993.

- Honjo, S., J. Dymont, W. Prell, and V. Ittekkot, Monsoon controlled export fluxes to the interior of the Arabian Sea, *Deep Sea Res., Part II*, 46, 1859–1902, 1999.
- Ittekkot, V., Particle flux studies in the Indian Ocean, *Eos Trans. AGU*, 72, 527–530, 1991.
- Ittekkot, V., The abiotically driven biological pump in the ocean and short-term fluctuations in atmospheric CO₂ contents, *Global Planet. Change*, 8, 17–25, 1993.
- Johnson, K. M., K. D. Wills, D. B. Butler, W. K. Johnson, and C. S. Wong, Coulometric total carbon dioxide analysis for marine studies: Maximizing the performance of an automated gas extraction system and coulometric detector, *Mar. Chem.*, 44, 167–187, 1993.
- Körtzinger, A., H. Thomas, B. Schneider, N. Gronau, L. Mintrop, and J. C. Duinker, At-sea intercomparison of two newly designed underway pCO₂ systems—Encouraging results, *Mar. Chem.*, 52, 133–145, 1996.
- Körtzinger, A., L. Mintrop, and J. C. Duinker, Strong CO₂ emissions from the Arabian Sea during South-West Monsoon, *Geophys. Res. Lett.*, 24, 1763–1766, 1997.
- Latasa, M., and R. R. Bidigare, A comparison of phytoplankton populations of the Arabian Sea during the Spring Intermonsoon and Southwest Monsoon of 1995 as described by HPLC-analyzed pigments, *Deep Sea Res., Part II*, 45, 2133–2170, 1998.
- Lendt, R., H. W. Bange, A. Hupe, H. Thomas, S. Al Habsi, S. Rapsomanikis, V. Ittekkot, and M. O. Andreae, Greenhouse gases in cold water filaments in the Arabian Sea during the Southwest Monsoon, *Naturwissenschaften*, 86, 489–491, 1999.
- Mantoura, R. F. C., C. S. Law, N. J. P. Owens, P. H. Burkill, E. M. S. Woodward, R. J. M. Howland, and C. A. Llewellyn, Nitrogen biogeochemical cycling in the northwestern Indian Ocean, *Deep Sea Res., Part II*, 40, 651–671, 1993.
- Naqvi, S. W. A., Some aspects of the oxygen-deficient conditions and denitrification in the Arabian Sea, *J. Mar. Res.*, 45, 1049–1072, 1987.
- Olson, D. B., G. L. Hitchcock, R. Fine, and B. A. Warren, Maintenance of the low-oxygen layer in the central Arabian Sea, *Deep Sea Res., Part II*, 40, 673–685, 1993.
- Owens, N. J. P., P. H. Burkill, R. F. C. Mantoura, E. M. S. Woodward, I. A. Bellan, J. Aiken, R. J. M. Howland, and C. A. Llewellyn, Size fractionated primary production and nitrogen assimilation in the NW Indian Ocean, *Deep Sea Res. Part II*, 40, 697–709, 1993.
- Quasim, S. Z., Biological productivity of the Indian Ocean, *Ind. J. Mar. Sci.*, 6, 122–137, 1977.
- Quasim, S. Z., Oceanography of the northern Arabian Sea, *Deep Sea Res., Part A*, 29, 1041–1068, 1982.
- Redfield, A. C., B. H. Ketchum, and F. A. Richards, The influence of organism on the composition of seawater, in *The Sea*, vol. 2, edited by M. N. Hill, pp. 26–77, Wiley-Interscience, New York, 1963.
- Sarma, V. V. S. S., M. Dileep Kumar, and M. D. George, The central and eastern Arabian Sea as a perennial source of atmospheric carbon dioxide, *Tellus, Ser. B*, 50, 179–184, 1998.
- Sellmer, C., Phytoplanktologische Studien im westlichen Arabischen Meer zur Zeit des SW-Monsuns—Ein Beitrag zum Verständnis des regionalen Kohlenstoffkreislaufs, *Ber. Inst. Meereskunde Christian-Albrechts-Univ. Kiel 309*, pp. 1–154, Kiel, Germany, 1999.
- Somasundar, K., A. Rajendran, M. Dileep Kumar, and R. Sen Gupta, Carbon and nitrogen budgets of the Arabian Sea, *Mar. Chem.*, 30, 363–377, 1990.
- Swallow, J. C., Some aspects of the physical oceanography of the Indian Ocean, *Deep Sea Res., Part A*, 31, 639–650, 1984.
- Thomas, H., V. Ittekkot, C. Osterroth, and B. Schneider, Preferential recycling of nutrients—The ocean's way to increase new production and to pass nutrient limitation?, *Limnol. Oceanogr.*, 44, 1999–2004, 1999.
- Wanninkhof, R., Relationship between wind speed and gas exchange over the ocean, *J. Geophys. Res.*, 97, 7373–7382, 1992.
- Wilkerson, F. P., and R. C. Dugdale, Silicate versus nitrate limitation in the equatorial Pacific estimated from satellite-derived sea-surface temperatures, *Adv. Space Res.*, 18, 81–89, 1996.
- Wyrtki, K., *Oceanographic Atlas of the International Indian Ocean Expedition*, Natl. Sci. Found., Washington, D. C., 1971.
- Zeitzschel, B., and S. A. Gerlach, *The Biology of the Indian Ocean*, 3rd ed., Springer-Verlag, New York, 1973.

A. Hupe, Institute of Biogeochemistry and Marine Chemistry, University of Hamburg, Bundesstrasse 55, D-20146 Hamburg, Germany.

V. Ittekkot, Centre for Tropical Marine Ecology, Fahrenheitstrasse 6, D-28539 Bremen, Germany.

R. Lendt and H. Thomas, Department of Marine Chemistry and Geology, Royal Netherlands Institute for Sea Research (NIOZ), P.O. Box 59, NL-1790 AB Den Burg, Texel, Netherlands. (hthomas@nioz.nl)